Optical Materials 72 (2017) 756–764

Contents lists available at ScienceDirect

Optical Materials

journal homepage: www.elsevier.com/locate/optmat

# Thermal radiation in one-dimensional photonic quasicrystals with graphene

C.H. Costa [a], M.S. Vasconcelos [b, *], U.L. Fulco [c], E.L. Albuquerque [c]

[a] Universidade Federal do Ceará, Campus Avançado de Russas, 62900-000, Russas, CE, Brazil
[b] Escola de Ciências e Tecnologia, Universidade Federal do Rio Grande do Norte, 59072-970, Natal, RN, Brazil
[c] Departamento de Biofísica e Farmacologia, Universidade Federal do Rio Grande do Norte, 59072-970, Natal, RN, Brazil

ARTICLE INFO

*Article history:*
Received 6 May 2017
Received in revised form
26 June 2017
Accepted 14 July 2017

*Keywords:*
Photonic band gap
Quasiperiodic structures
Thermal radiation
Graphene

ABSTRACT

In this work we investigate the thermal power spectra of the electromagnetic radiation through one-dimensional stacks of dielectric layers, with graphene at their interfaces, arranged according to a quasiperiodic structure obeying the Fibonacci (FB), Thue-Morse (TM) and double-period (DP) sequences. The thermal radiation power spectra are determined by means of a theoretical model based on a transfer matrix formalism for both normal and oblique incidence geometries, considering the Kirchhoff's law of thermal radiation. A systematic study of the consequences of the graphene layers in the thermal emittance spectra is presented and discussed. We studied also the radiation spectra considering the case where the chemical potential is changed in order to tune the omnidirectional photonic band gap.



## 1. Introduction

The search for optical materials exhibiting peculiar specific thermal emission properties has been driven on by the necessity of obtaining high-performance devices for light harvesting and thermal energy control. Therefore, devices displaying either very low or very high emissivity values over relatively broad frequency ranges are generally required. Unfortunately, there is no one natural material that is able to exhibit these properties and, hence, it is necessary to fabricate artificial ones for this purpose, a material engineering task.

One of the way to do this task consists in setting up a photonic crystal composed by an array of dielectric multilayers, where the resulting optical properties are not shared by their constituents. Photonic crystal is an artificial composite that affects the motion of photons in much the same way that ionic lattices affect electrons in solids. It exhibits the so-called photonic band gaps, ranges of frequency in which light cannot propagate through the structure irrespective of the propagation direction in space, in analogy with the energy bands and gaps in regular semiconductors [1,2]. They are created by spatial modulated dielectric functions in a periodic fashion in insulators, in which an electromagnetic field can be propagated with low loss, analogously to the periodic crystal potential electrons experience in a crystal. Several schemes for their fabrication have been proposed or realized so far, in which they exhibit both electric and magnetic resonances that can be separately tuned to occur from megahertz to terahertz frequency bands, and hopefully to the visible region of the electromagnetic spectrum [3]. Conventional photonic band gaps came from Bragg scattering in the photonic crystal, and can be modified by introducing different mechanisms, like quasiperiodic multilayers [4].

On the other hand, quasiperiodic multilayers are structures that can be classified as intermediate between ordered and disordered systems. Among the examples of quasiperiodic systems are the quasicrystals, which achieved prominence in 1984, following the report by Schechtman et al. of metallic Al-Mn alloys, showing amasing and interesting electron diffraction data [5]. For his discovery, D. Schechtman received the Nobel Prize in Chemistry in 2011. A fascinating feature of these structures is that they exhibit distinct physical properties, not found neither in periodic arrangements, nor in their constituent parts, giving rise to a novel description of disorder [6]. Quasicrystals, therefore, represent a special class of deterministic aperiodic structures exhibiting properties of self-similarity in their spectra [7,8], with a distinct appearance for each chain [9], even for different excitations [10–12]. A more recent precise and updated definition of

* Corresponding author.
*E-mail address:* mvasconcelosect@gmail.com (M.S. Vasconcelos).

http://dx.doi.org/10.1016/j.optmat.2017.07.029
0925-3467/

quasicrystals with dimensionality $n$ ($n = 1$, 2 or 3), is that in addition to their possible generation by a substitution process, they can also be formed from a projection of an appropriate periodic structure in a higher dimensional space $mD$, where $m > n$ [13].

The quasiperiodic structures choosen here are of the type generally known as substitutional sequences. Their scientific importance and significance can be measured by their investigation in several areas of mathematics [14], computer science [15], cryptography [16] and optics [17,18] to cite just a few. Besides, they are characterized by the nature of their Fourier spectrum, which can be dense pure points (as for the Fibonacci sequence) or singular continuous (as for the Thue-Morse and Double-period sequences) [19,20].

Another possibility to modify conventional photonic band gap is to intercalate a graphene layer between its interface [21–23]. Graphene is a flat monolayer of graphite with carbon atoms structured in a honeycomb geometry [24]. It has been considered a promising candidate material for the next generation of micro and nano-electronics devices (for a review see Ref. [25]). It has unintentionally been produced in small quantities for centuries through the use of pencils and other similar graphite applications, until being isolated and characterized by extracting single-atom-thick crystallites from bulk graphite in a groundbreaking experiment in 2004 [24]. The cleavage technique led directly to its first observation of the anomalous quantum Hall effect, providing direct evidence of graphene's theoretically predicted Berry's phase of massless Dirac fermions [26,27]. It is ultra-light yet immensely tough, being 200 times stronger than steel, although incredibly flexible. It is the thinnest material possible, a superb heat and electricity conductor and can act as a perfect barrier - not even helium can pass through it. Another of its main characteristic is the existence of Dirac cones in their electronic structure, resulting in structural and electronic properties with great potential to nano-electronics [28] and nanophotonics [29], besides an interesting optical response [30]. Furthermore, its reflectance, transmittance and absorbance are determined by fine-structure constant [31,32]. Despite of being only an atomic layer thickness with negligible reflection, a single free graphene layer shows significant absorbance in a near infrared range of the visible spectra [33]. In the infrared regime, the absorption of graphene can be tuned by applying gate voltages [34], making it a good candidate for transparent electrodes [35]. The absorption of broadband implies that graphene has also potential as an active medium for use in broadband photodetectors [36], ultra-fast lasers [37] and optical modulation [38]. In a general way these works have reported an unusual reflection, transmission and absorption spectra. In particular, a periodic stack of equally spaced parallel layers of graphene has the properties of a 1D photonic crystal, with narrow stop bands that are nearly periodic in frequency and a loss-independent density of optical states at the fixed lower-gap edges [39].

Until recently, no comprehensive analysis of these influences to the thermal radiation distribution appeared in the literature. Earlier works dealt with the alteration of stimulated emission rates due to cavity-confined blackbody radiation, giving physical results that differ from those in free space [40,41]. There are also few papers dealing with the quantum field description of photonic crystals related phenomena, such as the modification of spontaneous emission and the super-radiance effect [42,43], as well as the changes of the thermal radiation when it passed over a periodic and quasiperiodic (Cantor) multilayer structure incorporating either non-conventional (metamaterials) or conventional materials for both s- and p-polarizations [44].

To push further this field, our aim in this work is the investigation of the behavior of a light beam normally and obliquely incident on a one-dimensional multilayer photonic structure, composed of dielectric media with a graphene layer intercalated among them, looking for new efficient thermal emission devices. We consider the photonic structure arranged in a periodic as well as quasiperiodic fashion, following the Fibonacci (FB), Thue-Morse (TM), and double-period (DP) substitutional sequences (for an up to date review of these quasiperiodic structures see Ref. [45]). The main reason to study these structures, besides their scientific importance already mentioned above, is that they are realizable experimentally, so they are not mere academic examples of a quasicrystal. Furthermore, we intend to tailor the photonic band structures by considering the individual layers as quarter-wave layers, for which the photonic band gaps is expected to be more effective [46]. These quasiperiodic structures can be generated by their inflation rules, as follows: $A \to AB$, $B \to A$ (FB); $A \to AB$, $B \to BA$ (TM); $A \to AB$, $B \to AA$ (DP), respectively. Here, $A$ (thickness $d_A$) and $B$ (thickness $d_B$) are the building blocks modelling the $SiO_2$ and $TiO_2$ media, respectively. We use a theoretical model based on the Kirchhoff's law of thermal radiation to calculate the emission spectra of the thermal radiation in these multilayered structures, together with a transfer matrix formalism, which simplify enormously the algebra involved in the calculation.

The outline of this paper is as follows: in Sec. 2 we present the theoretical model based on the transfer matrix method together with the thermal radiation spectra in multilayered photonic structures. The numerical results are discussed in Sec. 3, while the conclusions are summarized in Sec. 4.

## 2. General theory

Consider the quasiperiodic multilayer structure, as depicted in Fig. 1. Medium $A$ ($B$), with thickness $d_A$ ($d_B$), is fulfilled by $SiO_2$ ($TiO_2$) and is characterized by the refractive index $n_A = \sqrt{\varepsilon_A} = 1.45$ ($n_B = \sqrt{\varepsilon_B} = 2.3$), with $\mu_A = 1$ ($\mu_B = 1$). The multilayer structure, whose unit cell is repeated $N$ times, is grown on an absorbing substrate $S$. The entire structure is surrounded by a transparent medium $C$ (considered to be vacuum) with a constant refractive index $n_C = 1$. The graphene layers, embedded between adjacent dielectric media, present a frequency dependent conductivity $\sigma_g(\omega)$ given by Refs. [47,48]:

$$\sigma_g(\omega) = \sigma_g^{intra}(\omega) + \sigma_g^{inter}(\omega), \tag{1}$$

with $\sigma_g^{intra}$ ($\sigma_g^{inter}$) being the intraband (interband) conductivity defined by:

$$\sigma_g^{intra}(\omega) = i\frac{e^2 k_B T}{\pi\hbar(\hbar\omega + i\Gamma)}\left[\frac{\mu_c}{k_B T} + 2\ln\left(e^{(-\mu_c/k_B T)} + 1\right)\right], \tag{2}$$

and

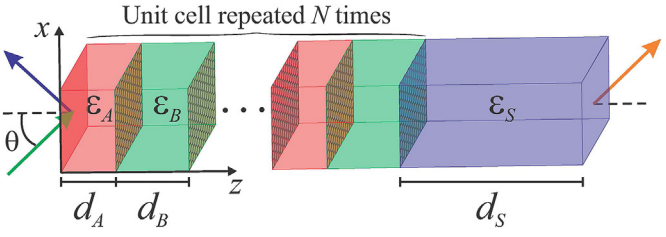


**Fig. 1.** The geometrical schematic representation of the multilayered photonic band gap structure considered in this work. The layers $A$ and $B$ have thicknesses $d_A$ and $d_B$, respectively, forming the building blocks of the whole quasiperiodic structure which are repeated $N$ times and are supported by an absorbing substrate of thickness $d_S$. We choose the incident and emergent media as vacuum, in which the total structure is embedded.

$$\sigma_g^{inter}(\omega) = i\frac{e^2}{4\pi\hbar}\ln\left[\frac{2|\mu_c| - (\hbar\omega + i\Gamma)}{2|\mu_c| + (\hbar\omega + i\Gamma)}\right]. \quad (3)$$

Here $e$ is the electronic charge, $\hbar = h/2\pi$ is the reduced Planck's constant, $k_B$ is the Boltzmann's constant, $T$ is the absolute temperature, $\Gamma$ is the damping constant of graphene and $\mu_c$ is the chemical potential, which can be controlled by a gate voltage.

To calculate the spectral properties of the one-dimensional optical quasiperiodic structures, i.e., the Fibonacci, Thue-Morse and double-period sequences, we can use a transfer matrix method [49,50]. This method relates the amplitudes of the electromagnetic fields in a layer with those of the former one, by successive applications of Maxwell's electromagnetic boundary conditions at each interface along the multilayer system. Therefore, the transfer matrix relates the electromagnetic incident field amplitudes ($A_{1C}^0$ and $A_{2C}^0$) of one side of the multilayer system (at $z<0$), with the transmitted amplitude $A_{1C}^N$ of the electromagnetic field in the other side, at $z>D$, $D$ being the size of the multilayer system (see Fig. 1), by means of the product of the interface matrices $M_{\alpha\beta}$ ($\alpha$, $\beta$ being any $A$, $B$, $S$ and $C$ media) and the propagation matrices $M_\gamma$ ($\gamma = A$, $B$ and $S$), as following [22,51]:

$$\begin{pmatrix} A_{1C}^0 \\ A_{2C}^0 \end{pmatrix} = M_{CA}M_AM_{AB}M_B\cdots M_{BS}M_SM_{SC}\begin{pmatrix} A_{1C}^N \\ 0 \end{pmatrix}, \quad (4)$$

where

$$M_{\alpha\beta}^{TE} = \frac{1}{2}\begin{bmatrix} 1+(1/k_{z\alpha})\left(k_{z\beta}+\sigma_g\mu_0\omega\right) & 1-(1/k_{z\alpha})\left(k_{z\beta}-\sigma_g\mu_0\omega\right) \\ 1-(1/k_{z\alpha})\left(k_{z\beta}+\sigma_g\mu_0\omega\right) & 1+(1/k_{z\alpha})\left(k_{z\beta}-\sigma_g\mu_0\omega\right) \end{bmatrix}, \quad (5)$$

for TE waves, and

$$M_{\alpha\beta}^{TM} = \frac{1}{2}\begin{bmatrix} 1+\left(k_{z\beta}/\varepsilon_\beta\right)\left[(\varepsilon_\alpha/k_{z\alpha})+(\sigma_g/\varepsilon_0\omega)\right] & 1-\left(k_{z\beta}/\varepsilon_\beta\right)\left[(\varepsilon_\alpha/k_{z\alpha})+(\sigma_g/\varepsilon_0\omega)\right] \\ 1-\left(k_{z\beta}/\varepsilon_\beta\right)\left[(\varepsilon_\alpha/k_{z\alpha})-(\sigma_g/\varepsilon_0\omega)\right] & 1+\left(k_{z\beta}/\varepsilon_\beta\right)\left[(\varepsilon_\alpha/k_{z\alpha})-(\sigma_g/\varepsilon_0\omega)\right] \end{bmatrix}, \quad (6)$$

for TM waves, with

$$M_\gamma = \begin{bmatrix} \exp(-ik_\gamma d_\gamma) & 0 \\ 0 & \exp(ik_\gamma d_\gamma) \end{bmatrix}. \quad (7)$$

Here $k_\gamma = n_\gamma\omega/c$, $k_x = (n_C\omega/c)\sin\theta$, $k_{z\gamma} = k_\gamma\cos\theta = [(n_\gamma\omega/c)^2 - k_x^2]^{1/2}$. Also, $c$ is the speed of the light in the vacuum and $\theta$ is the angle of the incident wave.

The transmittance and the reflectance coefficients are simply given, respectively, by

$$T(\omega) = \left|\frac{1}{M_{11}}\right|^2 \text{ and } R(\omega) = \left|\frac{M_{21}}{M_{11}}\right|^2, \quad (8)$$

where $M_{ij}$ ($i,j = 1,2$) are the elements of the optical transfer matrix $M(\omega) = M_{CA}M_AM_{AB}M_B\cdots M_{BS}M_SM_{SC}$. The general recurrence rules for the transfer matrix of the $n$-th generations of Fibonacci, Thue-Morse and double-period quasiperiodic sequences can be found in Ref. [17].

Few theories can describe directly the emissivity of a body, except for black bodies using Planck's radiation law, and the fundamental theory on spontaneous and induced emissions using the Einstein's coefficients. To circumvent this difficulty, the emissivity is usually calculated by an indirect argument that transforms an emission problem into a reflection problem. If no absorbing material is introduced in the multilayer system, i.e., if the refractive indices are all real (lossless), then $R(\omega) + T(\omega) = 1$ by conservation of energy. When we introduce a material with complex refractive index, i.e., the absorption is present, $R(\omega)$ and $T(\omega)$ can be used to define a real absorptance by $A(\omega) = 1 - R(\omega) - T(\omega)$, which is again a statement of conservation of energy. However, from Kirchhoff's law of thermal radiation, we know that the ratio of the thermal emittance $E(\omega)$ to the absorptance $A(\omega)$ is a constant, independent of the nature of the material, being the unity when the source is a perfect blackbody [52]. Hence, $E(\omega) = A(\omega)$ and therefore

$$E(\omega) = A(\omega) = 1 - R(\omega) - T(\omega). \quad (9)$$

Kirchhoff's law of thermal radiation has a long time controversy related to its range of validity. However, it seems well established, at least in the field of linear optics and in the case of elastic scattering. This is true even for macroscopic complex systems in nonthermal equilibrium with the surrounding radiation fields, provided the body is considered at uniform temperature, constant or varying very slowly. More precisely, provided the material quantum states of this body obey the equilibrium distribution, and the problems linked with the reflection reciprocity of the materials are taken into account.

Once the emittance is obtained, it is multiplied by the Planck's power spectrum $\rho^{BB}(\omega, T)$ to give the power spectrum of the quasiperiodic photonic structure. In this way, the power spectrum $\rho(\omega, T)$ of the layered structure in terms of its emittance $E(\omega)$, can be found to be

$$\rho(\omega, T) = E(\omega)\rho^{BB}(\omega, T), \quad (10)$$

with

$$\rho^{BB}(\omega, T) = \frac{\hbar\omega^3}{\pi^2c^2}[\exp(\hbar\omega/k_BT - 1)]^{-1}, \quad (11)$$

which is also known as Planck's law of blackbody radiation [53].

## 3. Numerical results

Considering the quasiperiodic multilayer structure in thermal equilibrium with its surroundings at a given absolute temperature $T$, we present now the numerical results for the spectral emissivity. Fundamentally, we want to know how the characteristic curve of the Planck's blackbody spectrum should be modified when we use a multilayered photonic crystal filter to model our physical system.

Let us assume the case in which both the magnetic permeability and the electric permittivity can be approximated by constants, for the same frequency range of interest. Furthermore, we assume the individual layers as quarter-wave layers, for which the quasiperiodicity is expected to be more effective, with the central

wavelength $\lambda_0 = 700$ nm [46]. These conditions yield the physical thickness in each layer defined by the following optical relation:

$$n_A d_A = n_B d_B = \lambda_0/4. \quad (12)$$

The phase shifts in the two layers are the same, i.e.,

$$\delta_A = (\pi/2)\Omega \cos(\theta_A), \quad (13)$$

$$\delta_B = (\pi/2)\Omega \cos(\theta_B), \quad (14)$$

where $\Omega = \omega/\omega_0 = \lambda_0/\lambda$ is the reduced frequency and the angles $\theta_A$ and $\theta_B$ are the incidence angles that the light beam makes with the normal of the layers ($z$-direction in Fig. 1). This multilayered photonic band gap stack is grown on an absorbing dielectric substrate characterized by a complex refractive index $n_S = 3.0 + i0.03$, whose thickness is given by $d_S = 100\lambda_0/n'_S$, $n'_S$ being the real part of $n_S$.

Fig. 2 presents the thermal radiation spectra (solid lines) for the periodic and some generations of the Fibonacci quasiperiodic structure, as a function of the reduced frequency $\Omega = \omega/\omega_0$, considering the normal incidence case with (red solid line) and without (blue solid line) graphene intercalated at the interfaces. In Fig. 2a we have the periodic case with 10 repetitions of the unit cell. Fig. 2b, c, d depict the quasiperiodic Fibonacci structure considering its third, fourth and fifth generations with $N = 8$, 6 and 5 repetitions, respectively. The normalized characteristic curves of the Planck's thermal radiation are represented by the dashed black line, meaning the perfect blackbody, while the spectra for an absorbing material with refractive index $n_S$ are represented by the dashed-dotted gray line. The absolute temperature $T$ is chosen so that the blackbody peak is aligned with the midgap frequency $\omega_0 = 2\pi c/\lambda_0$, which means a value approximately equal to 80 K. The main reason to choose this temperature is because in this range the effect of the so-called graphene-induced gap is better appreciated. At room temperature (300 K), for instance, this effect is minimal (not shown here). According to Ref. [54], the graphene sheets forming a parallel-plate waveguide may be used in photonic applications considering the chemical potential $\mu_c$ varying from 0 to 2 eV. For our numerical purpose the chemical potential was considered to be 0.2 eV. Observe that the Planck's curve profile for a perfect blackbody substrate represents the highest limit of the thermal emission of the multilayered sequences. In comparison with the curves related to the thermal emission for a non-ideal absorbing substrate (gray-body spectrum), the stacked thin-film photonic band gap structures arranged in a quasiperiodic way strongly alter its power

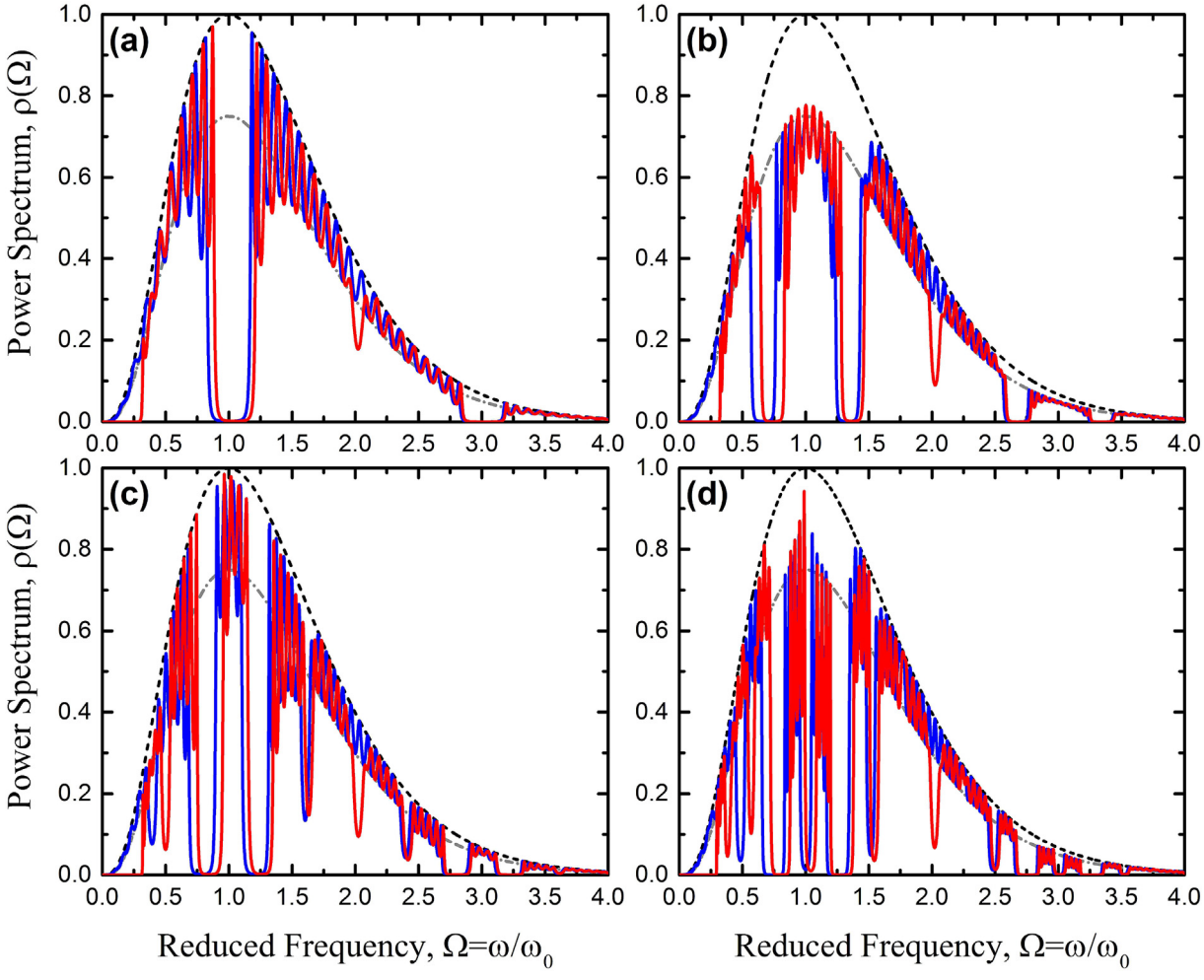


**Fig. 2.** The thermal radiation spectra (solid lines) as a function of the reduced frequency $\Omega = \omega/\omega_0$ considering the normal incidence case with (red solid line) and without (blue solid line) graphene. The normalized characteristic curves of Planck's thermal radiation are represented by dashed lines (the perfect blackbody). The dashed-dotted gray lines depict the spectra for an absorbing material with refractive index $n_S$. In all cases we consider the chemical potential $\mu_c = 0.2$ eV. The photonic multilayer structure is considered to be as follows: (a) a periodic structure, with $N = 10$ repetitions; (b) third; (c) fourth; and (d) fifth generations of the Fibonacci quasiperiodic structure, with $N = 8$; $N = 6$; and $N = 5$ repetitions, respectively. (For interpretation of the references to colour in this figure legend, the reader is referred to the web version of this article.)

spectrum, giving rise the so-called band gap structures (blue line spectrum).

For the periodic case (Fig. 2a) the thermal radiation spectrum presents a very soft behavior, without modulation, with higher values for $\rho(\Omega)$, when compared with the quasiperiodic cases. Observe the large band-gap around $\Omega = 1.0$, a kind of important signature of the periodic case with no counterpart in the quasiperiodic structures. If we move away from this band-gap region, the curve adjusts gradually towards the radiation emission profile of the gray-body spectrum.

Fig. 2b shows the thermal radiation spectrum for the third sequence of the Fibonacci quasiperiodic structure (up to the 2nd generation the spectrum is the same as in the periodic case). The spectrum presents now three band-gaps around the resonance frequencies $\Omega = 0.7, 1.3$ and 2.6, respectively, not as large as the one found around $\Omega = 1.0$, in the periodic case. Fig. 2c and d illustrate the effects on $\rho(\Omega)$ when one consider higher generations of the Fibonacci sequences, namely the fourth and fifth ones. As expected, the number of band-gaps increase according to the higher sequence chosen for the quasiperiodic structure (the same occurs also in Figs. 3 and 4 for the other quasiperiodic sequences). The reason for that is because when we increase the quasiperiodic generation number, more and more narrow localized modes appear as a consequence of a higher fragmentation of their internal energy profiles, characterizing the so-called Lebesgue measure of the energy spectrum (for a review see Ref. [6]).

When we intercalate a graphene layer among the interfaces (red line spectrum), we note that there is an additional large band gap in the lower frequency region $0 \leq \Omega \leq 0.31$ for the periodic and all Fibonacci generations. The physical origin of this band gap is only due to the existence of the graphene layers, giving rise to the so-called *graphene induced photonic band gap* (GIPBG). More specifically, using a transfer-matrix approach one can show that this photonic band gap is opened up as a consequence of a synergistic action of the Bragg scattering and the graphene conductance contributions [39]. The width of this gap strongly depends on the surface conductivity of the graphene and can be tuned via a gate voltage, so it can be used in the designing of tunable far-IR filters or switches. Of course, if the temperature is changed the quarter-wave parameters are changed too and, consequently, the effect of the graphene-induced gap is modified, be almost suppressed at the room temperature. Other much narrow GIPBG will appear for $\Omega = 2$, better appreciated when we vary the chemical potential $\mu_c$ on the emittance spectra (see Fig. 6).

Another interesting effect is associated to the slight shift of the localization of the band gaps due to the existence of a surface current induced by the modification of the electromagnetic boundary conditions caused by the presence of the graphene layers

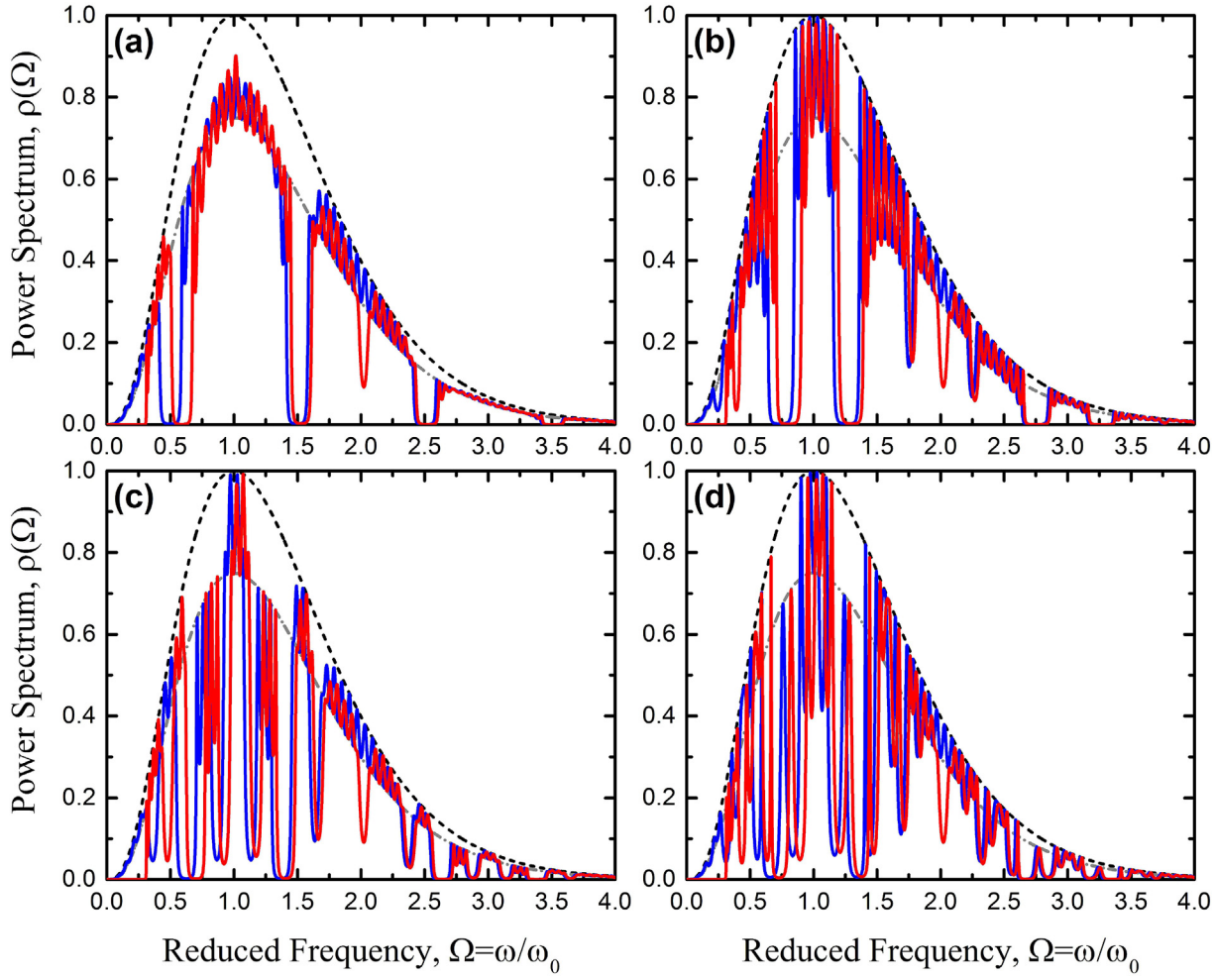


**Fig. 3.** Same as in Fig. 2, but considering the following Thue-Morse quasiperiodic generations: (a) second, with $N = 8$; (b) third, with $N = 4$; (c) fourth, with $N = 2$; and (d) fifth, with $N = 1$.

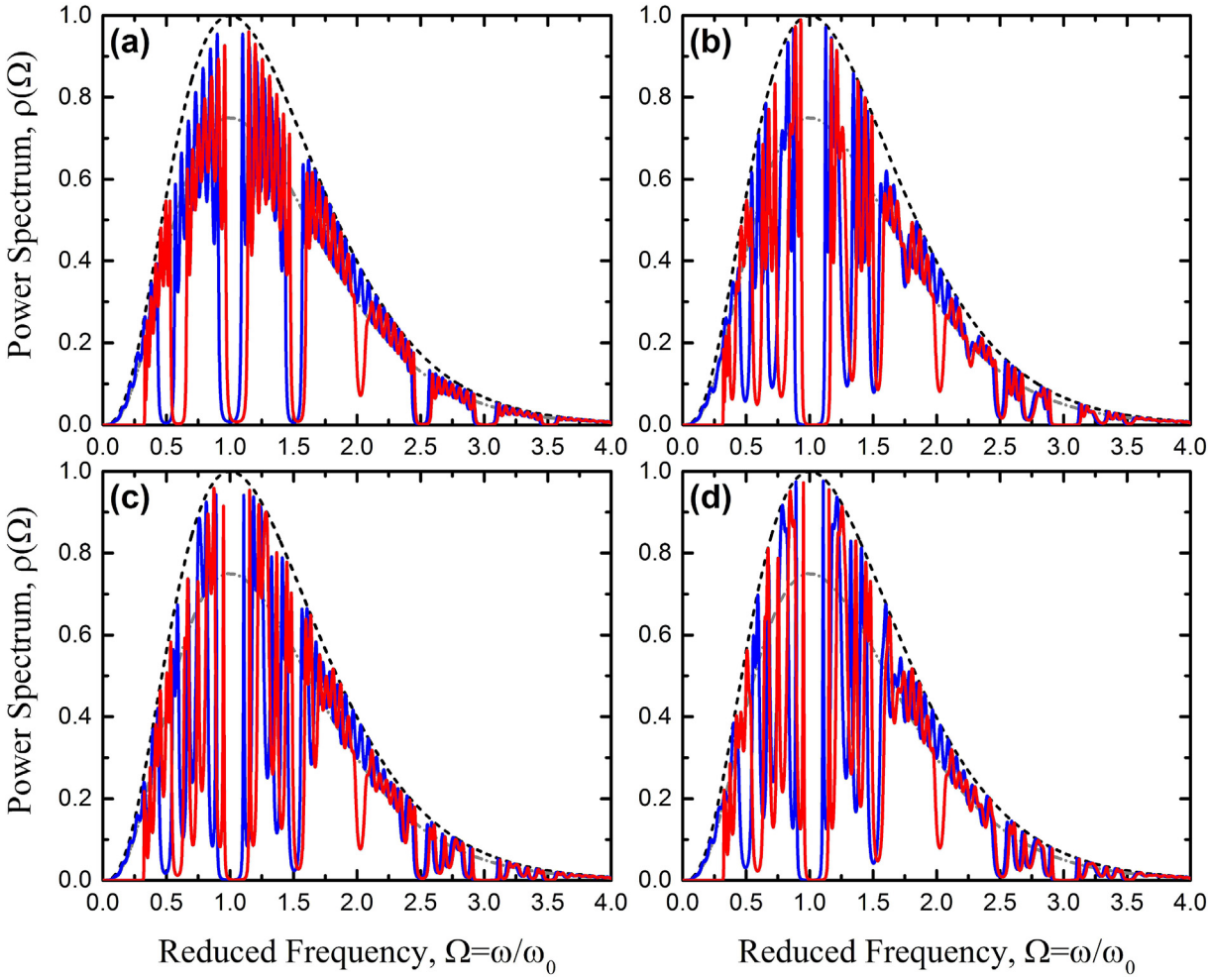


**Fig. 4.** Same as in Fig. 3, but considering the double period quasiperiodic sequence.

at the interfaces. Therefore the emission spectra, corresponding to the electromagnetic radiation emitted by the substrate $S$ and the thermal radiation spectrum, differ from the structure without graphene. The same effect in the transmission, refraction and absorption spectra have been observed in periodic [22], and quasiperiodic photonic crystals [23]. Furthermore, we observe that, for $\Omega > 2.5$, the power spectra with and without the graphene layers have the same profiles because the graphene conductivity is stronger in a low frequency regime, which is an expected result according to Eqs. (2) and (3).

Figs. 3 and 4 depict the thermal radiation spectra for some generations of the Thue-Morse (TM) and double-period (DP) quasiperiodic structures, namely (a) second generation, with $N = 8$; (b) third generation, with $N = 4$; (c) fourth generation, with $N = 2$; (d) fifth generation with $N = 1$. From these figures, besides the presence of the graphene induced band gap at low frequencies ($0 \leq \Omega \leq 0.31$), we can observe the presence of more common Bragg's gaps, making the power spectra richer regarding the possibilities to manipulate the light emission in theses systems. The reason for that lies in the way the sequences are built. Furthermore, for frequencies around the midgap, i.e., for $\Omega \cong 1$, we always obtained a Bragg band gap for the DP sequence, while for the TM case the emission coefficient reaches its maximum value.

The oblique incidence case of the thermal radiation spectra for periodic photonic crystal and third generations of Fibonacci, Thue-Morse and double-period photonic one-dimensional quasicrystals intercalated with graphene layers, are shown in Fig. 5, considering again the chemical potential $\mu_c = 0.2$ eV. The left (right) plots correspond to the TE (TM) polarization of the light beam. From this figure, we observe that the GIPBGs at the frequency range $0 \leq \Omega \leq 0.31$ are omnidirectional photonic band gaps, i.e., a frequency region that light can not propagate through the multilayered dielectric structures regardless of the incidence angle and/or the light polarization (black rectangles). However, they have different origins than the common omnidirectional Bragg's photonic bands gap, which is observed only for the periodic case (highlighted by the thin green rectangle; see Fig. 5a), since they are produced by Bragg's reflections arising due to the presence of the graphene layers at the interfaces. We also find that these GIPBGs are insensitive to the periodic or quasiperiodic arrangement of the photonic crystals.

Finally, we also investigate the influence of the chemical potential $\mu_c$ on the emittance spectra of the photonic quasicrystals studied here, depicted in Fig. 6 for normal incidence. From there one can note that besides the low-frequency GIPBGs, there are also a much narrow another one at $\Omega = 2$, both of them, as conjectured, strongly dependent on the chemical potential, which can be tuned by a gate voltage [55]. They are shifted toward higher frequencies when the chemical potential increases, in a opposite way of the conventional Bragg's ordinary photonic band gaps, highlighted by

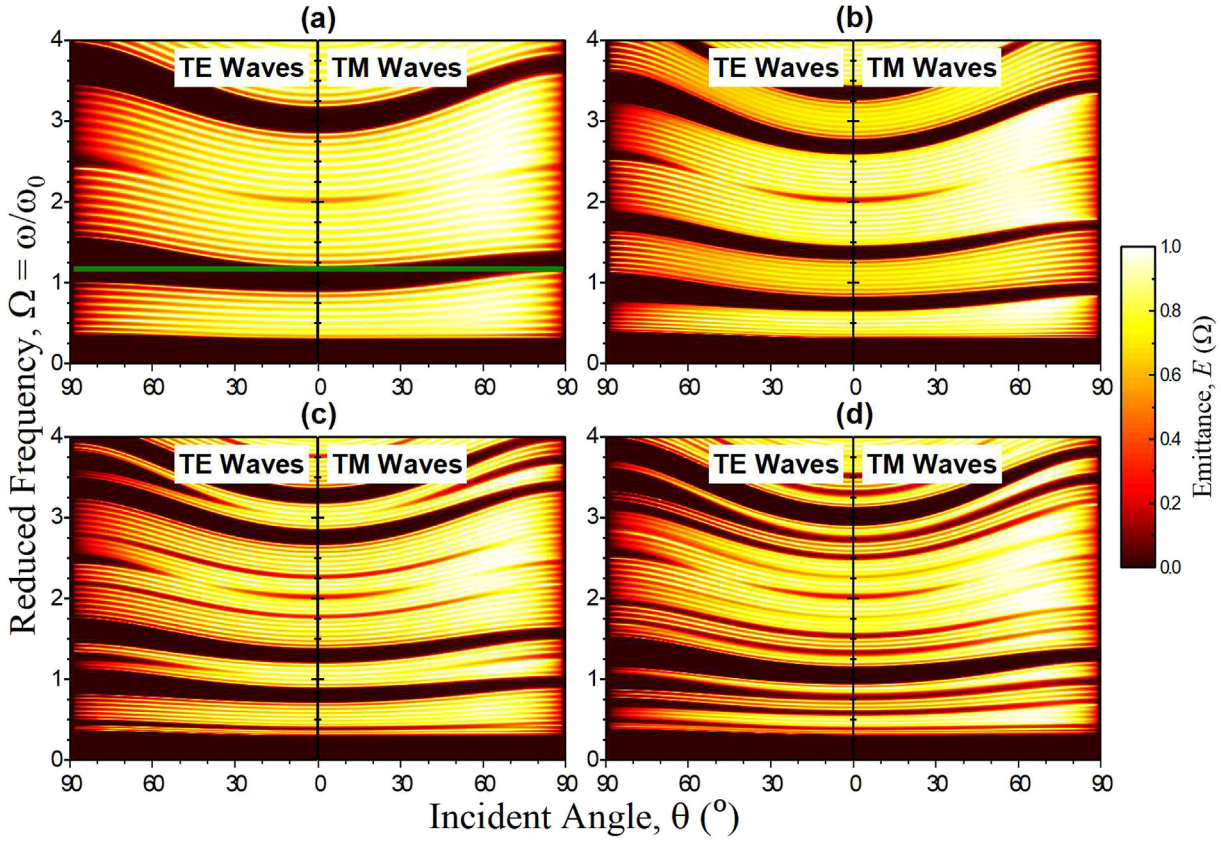


**Fig. 5.** Emittance spectra as a function of the reduced frequency $\Omega = \omega/\omega_0$ and the incident angle $\theta$ for: (a) a periodic structure, with $N = 10$; third generations of (b) Fibonacci ($N = 8$); (c) Thue-Morse ($N = 4$); and (d) double-period ($N = 4$) quasiperiodic sequences. The left- (right-) hand side is related to the TE (TM) polarization of the light beam.

the blue rectangles, which are not affected as predictable. The reason for that lies in the dependence on the chemical potential of the graphene surface conductances (Eqs. (2) and (3)). As shown in Ref. [58], an increasing of the chemical potential implies a shift to high frequencies of the conductance curve.

## 4. Conclusions

Looking for alternatives to set up a specific thermal emission device, we have investigated in this work the thermal behavior of light waves considering periodic and quasiperiodic photonic structures intercalated with graphene at their interfaces, namely those obeying the recursion relation which defines the Fibonacci, Thue-Morse and double-period sequences. Our results shows, in a general way, that the thermal spectra can be used for the enhancement, suppression or attenuation of the light in all or certain directions, by changing either the density of modes (or frequency), or the angle of incidence of the light, being important in the design of filters for modification of Planck's blackbody spectrum.

Our tailored photonic crystal can act either as a passive filter, where the refractive indices of each layers are real (i.e., low loss materials), or as an active emitter, where at least one of the layers in the photonic crystal has an imaginary refraction index. In both cases, the resulting thermal radiation spectrum of the photonic structure was substantially modified as compared to those corresponding to the original substrate alone, due to resonance effects within the photonic crystal.

In fact, in periodic photonic crystal the system blocks heat radiation emitted by the substrate at the frequencies corresponding to the photonic crystal band gap, and the substrate's emission is enhanced from the gray-body level all the way up to the perfect blackbody rate at a number of frequencies corresponding to the pass-band transmission resonances of the photonic crystal [56]. A similar enhancement of the substrate's thermal emittance at certain resonance frequencies, accompanied by a fragmented pass and stop-bands, due to the fractal nature of their transmission profiles [45], is observed in the Fibonacci quasiperiodic photonic crystal [56]. An analogous result is observed also in the thermal spectrum corresponding to the Thue-Morse quasiperiodic photonic crystal, whereas those corresponding to the double-period sequence is more similar to the periodic one around the midgap (or the band gap in periodic photonic system) of the spectral range. A very interesting fact is that these spiky thermal emission spectra can be substantially smoothed (hence obtaining broader spectral ranges with enhanced emittance) by using metamaterials in the composition of their individual layers [44,57].

The presence of the graphene layers give rise also of the so-called graphene induced photonic band gap (GIPBG), an additional chemical potential dependent narrow band gap in the lower frequencies range, for all sequences studied here. Besides, the localization of the band gaps are shifted toward higher frequencies, when compared to the same structure without the graphene layers, due to the existence of a surface current on the structure's interfaces. Moreover, only in the periodic case the emittance spectra have an ominidirectional band gap in the frequency region close to $\Omega \sim 1$.

So far, photonic band gap materials have already found a myriad of applications to mold the flow of light, e.g., novel waveguides, photonic crystal fibers, microcavities, photonic crystal lasers, to

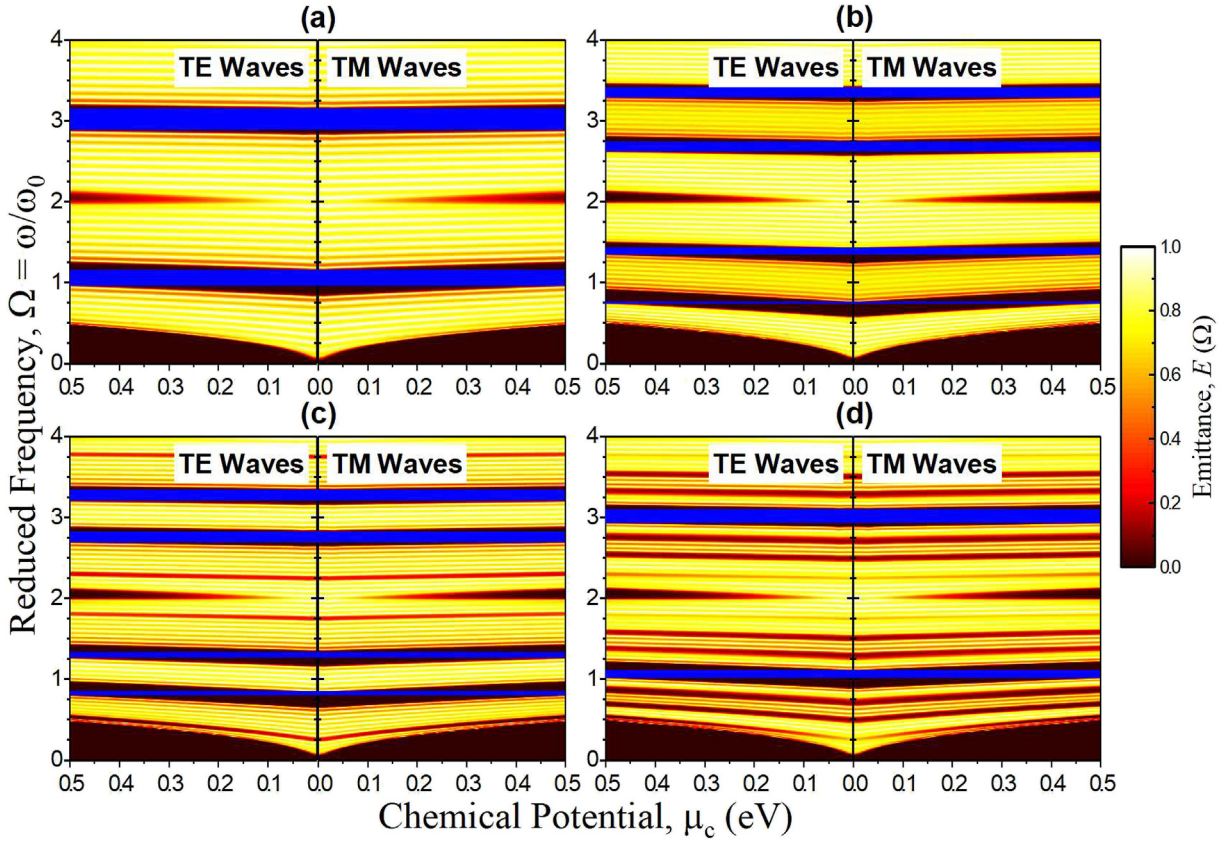


**Fig. 6.** Same as in Fig. 5 but for emittance spectra as a function of the reduced frequency $\Omega = \omega/\omega_0$ and the chemical potential $\mu_c$.

name just a few. On the other hand, thermal emission devices, as those proposed here, are still exploiting their way as important tools in the technological market. We hope our findings may help future works in this direction.

## Acknowledgments

We would like to thank partial financial support from the Brazilian Research Agencies CNPq and CAPES.

## References

[1] E. Yablonovitch, Phys. Rev. Lett. 58 (1987) 2059.
[2] S. John, Phys. Rev. Lett. 58 (1987) 2486.
[3] C.M. Soukoulis, M. Kafesaki, E.N. Economou, Adv. Mater. 18 (2006) 1941.
[4] M.S. Vasconcelos, E.L. Albuquerque, Phys. B 222 (1996) 113.
[5] D. Shechtman, I. Blech, D. Gratias, J.W. Cahn, Phys. Rev. Lett. 53 (1984) 1951.
[6] E.L. Albuquerque, M.G. Cottam, Phys. Rep. 376 (2003) 225.
[7] C.G. Bezerra, J.M. de Araujo, C. Chesman, E.L. Albuquerque, Phys. Rev. B 60 (1999) 9264–9267.
[8] E.L. Albuquerque, U.L. Fulco, V.N. Freire, E.W.S. Caetano, M.L. Lyra, F.A.B.F. Moura, Phys. Rep. 535 (2014) 139–209.
[9] P.M.C. de Oliveira, E.L. Albuquerque, A.M. Mariz, Phys. A 227 (1996) 206–212.
[10] E.L. Albuquerque, M.G. Cottam, Solid State Commun. 81 (1992) 383–386.
[11] C.G. Bezerra, E.L. Albuquerque, Phys. A 255 (1998) 285–292.
[12] D.H.A.L. Anselmo, M.G. Cottam, E.L. Albuquerque, J. Phys. Condens. Matter 12 (2000) 1041–1052.
[13] Z.V. Vardeny, A. Nahata, A. Agrawal, Nat. Photonics 7 (2013) 177.
[14] G. Christol, T. Kamae, M. Mendes-France, G. Rauzy, Bull. Soc. Math. Fr. 108 (1980) 401.
[15] A. Cobham, Math. Syst. Theory 6 (1972) 164.
[16] G.T. Herman, G. Hozenberg, Developmental Systems and Languages, 1975. North-Holland, Amsterdam.
[17] C.A.A. Araújo, M.S. Vasconcelos, P.W. Mauriz, E.L. Albuquerque, Opt. Mater. 35 (2012) 18–24.
[18] M.S. Vasconcelos, E.L. Albuquerque, Phys. Rev. B 59 (1999) 11128.
[19] M. Queffélec, Substitution Dynamical Systems: Spectral Analysis, Lecture Notes in Mathematics, vol. 1294, Springer-Verlag, Heidelberg, 1987.
[20] F. Axel, J.P. Allouche, Z.Y. Wen, J. Phys. Condens. Matter 4 (1992) 8713.
[21] A. Ferreira, J. Viana-Gomes, Y.V. Bludov, V.M. Pereira, N.M.R. Peres, A.H. Castro Neto, Phys. Rev. B 84 (2011) 235410.
[22] T. Zhan, X. Shi, Y. Dai, X. Liu, J. Zi, J. Phys. Condens. Matter 25 (2013) 215301.
[23] Y. Zhang, Z. Wu, Y. Cao, H. Zhang, Opt. Commun. 338 (2015) 168.
[24] K.S. Novoselov, A.K. Geim, S.V. Morozov, D. Jiang, Y. Zhang, S.V. Dubonos, I.V. Grigorieva, A.A. Firsov, Science 306 (2004) 666.
[25] A.H. Castro Neto, F. Guinea, N.M.R. Peres, K.S. Novoselov, A. Geim, Rev. Mod. Phys. 81 (2009) 109.
[26] K.S. Novoselov, A.K. Geim, S.V. Morozov, D. Jiang, M.I. Katsnelson, I.V. Grigorieva, S.V. Dubonos, A.A. Firsov, Nature 438 (2005) 197.
[27] Y. Zhang, Y.W. Tan, H.L. Stormer, P. Kim, Nature 438 (2005) 201.
[28] S.H.R. de Sena, J.M. Pereira Jr., G.A. Farias, M.S. Vasconcelos, E.L. Albuquerque, J. Phys. Condens. Matter 22 (2010) 465305.
[29] F. Javier García de Abajo, Science 339 (2013) 917.
[30] C. Lee, J.Y. Kim, S. Bae, K.S. Kim, B.H. Hong, E.J. Choi, Appl. Phys. Lett. 98 (2011) 071905.
[31] K.F. Mak, M.Y. Sfeir, Y. Wu, C.H. Lui, J.A. Misewich, T.F. Heinz, Phys. Rev. Lett. 101 (2008) 196405.
[32] R.R. Nair, P. Blake, A.N. Grigorenko, K.S. Novoselov, T.J. Booth, T. Stauber, N.M.R. Peres, A.K. Geim, Science 320 (2008) 1308.
[33] T. Stauber, N.M.R. Peres, A.K. Geim, Phys. Rev. B 78 (2008) 085432.
[34] Z.Q. Li, E.A. Henriksen, Z. Jiang, Z. Hao, M.C. Martin, P. Kim, H.L. Stormer, D.N. Basov, Nat. Phys. 4 (2008) 532.
[35] S. Bae, H. Kim, Y. Lee, X. Xu, J.S. Park, Y. Zheng, J. Balakrishnan, T. Lei, H.R. Kim, Y.I. Song, Y.J. Kim, K.S. Kim, B. Özyilmaz, J.H. Ahn, B.H. Hong, S. Iijima, Nat. Nanotechnol. 5 (2010) 574.
[36] T. Stauber, G. Gómez-Santos, Phys. Rev. B 85 (2015) 075410.
[37] Z. Sun, T. Hasan, F. Torrisi, D. Popa, G. Privitera, F. Wang, F. Bonaccorso, D.M. Basko, A.C. Ferrari, ACS Nano 4 (2010) 803.
[38] M. Liu, X. Yin, E. Ulin-Avila, B. Geng, T. Zentgraf, L. Ju, F. Wang, X. Zhang, Nature 474 (2011) 64.
[39] Y. Fan, Z. Wei, H. Li, H. Chen, C.M. Soukoulis, Phys. Rev. B 88 (2013) 241403R.
[40] K.S. Lai, E.A. Hinds, Phys. Rev. Lett. 81 (1998) 2671.
[41] C.M. Cornelius, J.P. Dowling, Phys. Rev. A 59 (1999) 4736.
[42] J. Kästel, M. Fleischhauer, Phys. Rev. A 71 (2005) 01180.
[43] J. Kästel, M. Fleischhauer, Laser Phys. 15 (2005) 1.
[44] M. Maksimović, Z. Jaksić, J. Opt. A Pure Appl. Opt. 8 (2006) 355.
[45] E.L. Albuquerque, M.G. Cottam, Polaritons in Periodic and Quasiperiodic Structures, Elsevier, Amsterdam, 2004.

[46] M.S. Vasconcelos, E.L. Albuquerque, A.M. Mariz, J. Phys. Condens. Matter 10 (1998) 5839.
[47] S.H. Abedinpour, G. Vignale, A. Principi, M. Polini, W.-K. Tse, A.H. MacDonald, Phys. Rev. B 84 (2011) 045429.
[48] F.H.L. Koppens, D.E. Chang, F.J. Garcia de Abajo, Nano Lett. 11 (2011) 3370.
[49] E.L. Albuquerque, P. Fulco, G.A. Farias, M.M. Auto, D.R. Tilley, Phys. Rev. B 43 (1991) 2032–2041.
[50] M.S. Vasconcelos, E.L. Albuquerque, Phys. Rev. B 59 (1999) 11128.
[51] F.F. de Medeiros, E.L. Albuquerque, M.S. Vasconcelos, J. Phys. Condens. Matter 18 (2006) 8737.
[52] P. Pigeat, D. Rouzel, B. Weber, Phys. Rev. B 57 (1998) 9293.
[53] M. Planck, The Theory of Heat Radiation, Dover, New York, 1959.
[54] G.W. Hanson, J. Appl. Phys. 104 (2008) 084314.
[55] L. Zhang, G. Wang, X. Han, Y. Zhao, Optik 127 (2016) 2030.
[56] F.F. de Medeiros, E.L. Albuquerque, M.S. Vasconcelos, P.W. Mauriz, J. Phys. Condens. Matter 19 (2007) 496212.
[57] E. Maciá, Nanomaterials 5 (2015) 814–825.
[58] A. Madania, S.R. Entezar, Phys. B 431 (2013) 1.